Conduction of DNA molecules attached to a disconnected array of metallic Ga nanoparticles

2011 New J. Phys. 13 063046

(http://iopscience.iop.org/1367-2630/13/6/063046)

New Journal of Physics
The open-access journal for physics

Conduction of DNA molecules attached to a disconnected array of metallic Ga nanoparticles

A D Chepelianskii[1], D Klinov[2], A Kasumov[1], S Guéron[1], O Pietrement[3], S Lyonnais[4] and H Bouchiat[1,5]

[1] Université Paris-Sud, CNRS, UMR 8502, F-91405 Orsay, France
[2] Shemyakin-Ovchinnikov Institute of Bioorganic Chemistry, Russian Academy of Sciences, Miklukho-Maklaya 16/10, Moscow 117871, Russia
[3] UMR 8126 CNRS-IGR-UPS, Institut Gustave-Roussy, 39 rue Camille Desmoulins, 94805 Villejuif Cedex, France
[4] Museum National d'Histoire Naturelle, CNRS, UMR7196, Inserm, U565, 43 rue Cuvier, 75005 Paris, France
E-mail: bouchiat@lps.u-psud.fr

New Journal of Physics **13** (2011) 063046 (10pp)
Received 10 December 2010
Published 29 June 2011
Online at http://www.njp.org/
doi:10.1088/1367-2630/13/6/063046

Abstract. We have investigated the conduction over a wide range of temperatures of λ DNA molecules deposited across slits etched through a few-nanometers-thick platinum film. The slits were insulating before DNA deposition but contained metallic Ga nanoparticles, a result of focused ion beam etching. When these nanoparticles were superconducting, we found that they can induce superconductivity through the DNA molecules, even though the main electrodes are nonsuperconducting. These results indicate that minute metallic particles can easily transfer charge carriers to attached DNA molecules and provide a possible reconciliation between apparently contradictory previous experimental results concerning the length over which DNA molecules can conduct electricity.

[5] Author to whom any correspondence should be addressed.

Contents

1. Introduction

Conductivity of DNA is a topic of long-standing debate. Following initial predictions that DNA molecules should conduct electricity, several types of experiments were attempted to probe the conduction mechanisms, ranging from emission and absorption spectroscopies [1] to microwave absorption [2]. Several groups have also attempted direct measurements of DNA conductivity by attaching DNA molecules to metallic electrodes [3, 4]. The contradictory experimental results, with behavior ranging from insulator to coherent quantum transport over distances in the 100 nm range, led to strong controversy [5]. The picture emerging over the last few years has been that DNA can conduct over distances of tens of nanometers: this was shown by scanning tunneling microscopy and local probe techniques [7–10], as well as in a spectacular experiment [6]: a 3 nm-long DNA molecule was inserted in a cut carbon nanotube, increasing its initial resistance only twofold, and was subjected to biological manipulations that altered and then restored the conductivity. The importance of the environment of the molecules for obtaining reproducible results was pointed out in [14]. Conduction over hundreds of nanometers, and up to several microns, was also reported by different groups [3, 11–13], including ours. In our previous experiments, DNA was found to be conductive between platinum and carbon electrodes [16] and between rhenium and carbon electrodes [15]. In this last case, as the temperature was lowered below the superconducting critical temperature of the electrodes (rhenium is a superconductor with $T_c = 1.7$ K) the sample resistance decreased, indicating coherent quantum transport through the DNA molecules. These results are both technologically and fundamentally important since long-range transport in DNA molecules may lead to the creation of new nanoscale self-assembled electronic devices. From a fundamental point of view, DNA is one of the rare one-dimensional molecular wires that can be obtained in mono dispersed form with known chemical structure and chirality. It is thus important to understand the ingredients that lead to conduction over long distances.

In this paper, we reconcile previous findings by showing that conduction over distances greater than hundreds of nanometers can occur if the DNA molecules are attached to a disconnected array of nanoparticles (typically 10–20 nm apart) that induce charge carriers through the molecules, enhancing conduction. In addition, in our case the nanoparticles are superconducting, which induces superconducting correlations in DNA at low temperatures.

2. Sample fabrication

All our samples, including the previous ones, are made with unconventional techniques: without electron beam lithography and with functionalization of the sample surface by a pentylamine plasma before deposition of DNA molecules. In the following, we detail the different steps of the fabrication using focused ion beam (FIB) etching of a thin platinum carbon film deposited on mica, with subsequent pentylamine plasma treatment.

2.1. Fabrication of the electrodes for the investigation of DNA transport

Fabrication begins with a mica substrate covered by an e-gun-deposited platinum carbon film a few nanometers thick (5 nm thick, square resistance 1 kΩ). We deposit thick gold contact pads through a mechanical mask and divide the centimeter square mica substrate into roughly 12 sample regions using a UV laser with a 30 μm diameter laser beam; see figure 1. We then proceed to etch away the metal over a thin, 50 μm long region using an FIB of Ga ions (magnification $\times$3000 and current 3.5 pA). In order to obtain narrow insulating regions, we monitor the resistance of a first slit as we etch the platinum film one line scan at a time. We stop the etching as soon as the resistance diverges; see figure 1. The other slits are etched using a slightly larger (15%) number of scans than was necessary to open the first slit. We then check electrically with a probe station that all slits have a resistance above a few GΩ. The width of the slits fabricated with this technique ranges between 70 and 150 nm. We have used both atomic force microscopy (AFM) and high-resolution scanning electron microscopy to characterize the structure of the FIB etched slit. We find that the insides of the slits are rather rough for two reasons: the incomplete etching of the platinum/carbon film leaves metallic disconnected islands of typical size 10 nm; see figure 2. In addition, some slits contain a disordered array of roughly spherical nanoparticles (see figure 3). The regular shape of these spheres contrasts with the irregular shape of the etching residues of Pt/C. As confirmed by transport experiments presented below, these spherical nanoparticles result from condensed gallium droplets generated by the FIB. Their size varies between 3 and 10 nm and their separation between 5 and 20 nm. Even if these nanoparticles do not directly contribute to electronic transport through the slits, which are insulating before deposition of DNA and remain so after a flow of saline buffer solution without molecules, we will see that they modify the electronic properties of DNA molecules deposited across the slit.

2.2. Functionalization of the samples with pentylamine

Just before deposition of DNA molecules, the substrates are functionalized in a dc arc discharge plasma with pentylamine vapor pressure $P = 0.1$ torr and current $I = 3$–5 mA for a few minutes. Pentylamine was used because it is known to promote attachment of DNA to amorphous carbon films (such as those used in transmission electron microscopy, see [17]). Compared to our previous experiments we have gained a better understanding of this functionalization technique, establishing that pentylamine adheres only on carbonated surfaces and not directly on mica or metals. Although the carbon concentration in the Pt/C film constituting the electrodes is not known exactly, we checked that this concentration was high enough to anchor the pentylamine, since no DNA was attached to a platinum surface without co-deposited carbon. The pentylamine plasma [17] creates a positively charged organic

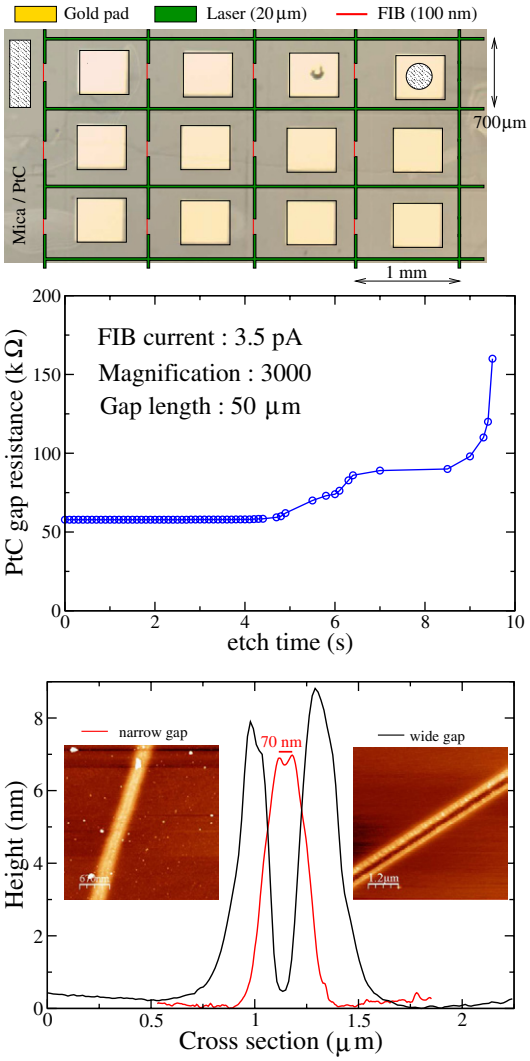

Figure 1. Top panel: general view of the samples showing the macroscopic gold pads on the Pt/C film with the laser and FIB etched slits. Medium panel: resistance of a gap during FIB etching as a function of exposure time. The gap is etched in a single scan mode with a scan time of 0.1 s, which allows us to measure the resistance after each scan. After total time $t > 9.7$ s, the resistance jumps and the gap becomes insulating. Bottom panel: averaged height profile from two gaps prepared using an FIB; their atomic force microscopy (AFM) images are shown in the color insets. The narrow gap was obtained during the calibration resistance measurement from figure 1, whereas the wide gap was obtained with a larger exposure time. The width of the insulating region is hard to measure precisely with AFM because of the residues produced during etching, which accumulate at the edges of the slit.

layer constituted by amine groups of various sizes that allows DNA molecules to bind to the carbonated hydrophobic electrodes. Conducting AFM characterization of this pentylamine layer on a smooth Pt/C film indicates that the pentylamine film forms a smooth insulating layer. This is not the case along the edge of the slits, where FIB etching as well as unavoidable carbon

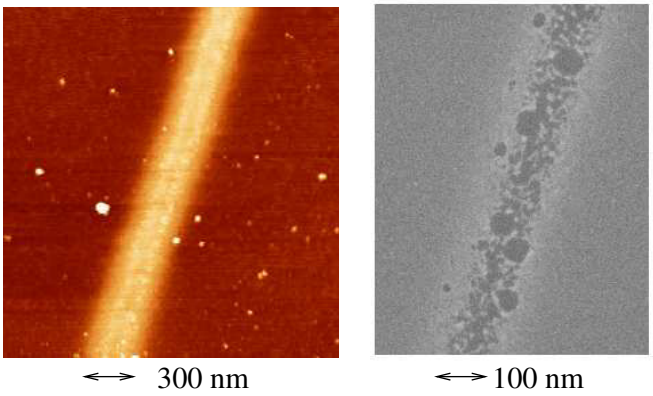

Figure 2. AFM image (left) and scanning electron microscopy image (right) of a typical slit after FIB etching. The slit is electrically insulating but metallic islands and filaments are clearly visible in the etched region.

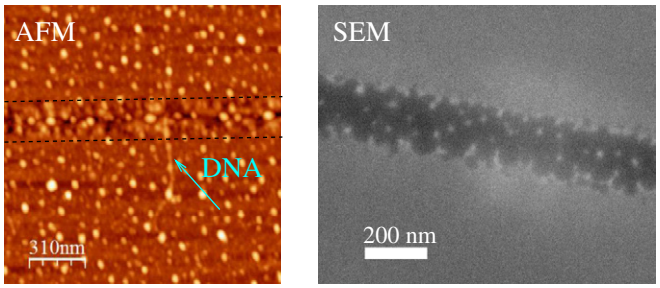

Figure 3. Left panel: AFM image of one of the samples where low-temperature transport was investigated, taken using an ultra-sharp AFM tip and showing the presence of a DNA molecule across the slit. The slit is nearly invisible due to the scanning direction chosen to be parallel to the slit in order to optimize the DNA visualization. Right panel: scanning electron microscopy image of the same sample. Gallium nanoparticles are clearly visible in the etched slit region.

contamination introduces roughness, leading to defects and holes in the pentylamine coverage. As a result the edges of the slit remain metallic, as is needed to establish electrical contact to the DNA on both sides of the slit.

2.3. DNA deposition and characterization

A drop of λ-DNA[6] solution was incubated on the substrate surface for a few minutes and then rinsed away using a water flow created by a peristaltic pump (flow: a few $\mathrm{cm\,s^{-1}}$). Out of eight mica substrates treated independently with pentylamine and on which DNA deposition

[6] The λ DNA solution ($5\,\mu\mathrm{g\,ml^{-1}}$) was prepared with a commercial solution, 'Invitrogen Cat. no. 25250-028' ($250\,\mu\mathrm{g\,ml^{-1}}$), in Tris-HCl $(\mathrm{HOCH_2})_3\,\mathrm{CNH_2} + \mathrm{HCl}$ (pH 7.4), 10 mM NaCl and 5 mM EDTA 0.1 mM diluted in a magnesium chloride buffer $\mathrm{CH_3COO^-} + \mathrm{NH_4^+}$ (15 mM) and $\mathrm{MgCl_2}$ (5 mM).

Table 1. Success rates for the formation of conductive junctions by deposition of λ molecules. All substrates were treated independently for pentylamine deposition. It is important to note that on the same substrate, samples are either all insulating or nearly all conducting after deposition of DNA.

Number of substrates	12
Number of FIB slits	$\simeq 100$
Number of substrates with visible λ DNA	5
Number of substrates with conducting slits after λ deposition	3
Number of slits on these three substrates	15
Number of conducting slits after λ deposition	11
Number of slits on the control sample	14
Number of conducting slits after buffer	0

was attempted using the procedure described above[7], five were covered by DNA molecules as established by AFM. These five substrates contained around 30 slits. All samples on two of these substrates were completely insulating. On the other three substrates, 11 out of 15 samples were conducting. We have also prepared a control substrate, incubated with the same buffer but without DNA molecules, and rinsed like the other samples. We found that all 14 slits etched on these samples remained insulating after incubation in the sole buffer solution. Room temperature conductance was measured in a probe station, using an ac voltage in the mV range at frequencies ranging from 0 to 30 Hz. The resistance of conducting samples was found to vary, depending on the slit, between 5 and 50 kΩ. These values are consistent with previous findings [15, 16], given that the number of deposited molecules across each slit varies between 10 and 100. (See table 1)

3. Low-temperature measurements

In the following, we present low-temperature transport measurements of DNA molecules deposited across slits decorated with gallium nanoparticles. The samples investigated have resistances ranging from 5 to 20 kΩ at room temperature, with roughly 10–30 connected molecules, as deduced from the density of molecules on the substrate far from the slit. The samples were electronically and mechanically connected by gold-plated spring contacts[8] on the gold pads on the Pt/C film, and mounted in a dilution refrigerator operating down to 50 mK. The resistance was measured via lines with room-temperature low-pass filters. In order to optimize the signal-to-noise ratio, these measurements were carried out in a current biased configuration using an ac current source of 1 nA operating at 27 Hz and a lock-in detector with a low-noise voltage pre-amplifier. This frequency is chosen low enough in order that the signal measured is dominated by the resistive part of the sample without any detectable out of phase contribution coming from the capacitances of the measurement circuit. Whereas the resistance was nearly

[7] Plasma functionalization and DNA deposition were attempted at two different laboratories, but conducting samples were obtained only in the setup in Moscow. Thus electrical measurements were carried out in Orsay several days later.

[8] Standard connecting techniques such as ultrasonic or silver paste bonding destroyed the conductivity of most of the samples.

independent of temperature between room temperature and 4 K, it dropped as T decreased, with a broad transition to a value $R_{\min}$ of the order of 4 kΩ. We attribute this transition to proximity superconductivity induced through the DNA molecules by Ga nanoparticles. The residual resistance $R_{\min}$ corresponds to the resistance of the normal Pt/C electrodes. Note that whereas these low-temperature data are shown only in two particular samples, similar behavior was found in the case of all five samples measured on the chip.

Another superconducting-like feature is the nonlinear IV curves at low temperature. The differential resistance as a function of dc current is measured by adding a dc current to the small 1 nA ac current. This quantity is depicted in figure 5 as a function of the dc current $I_{\rm dc}$. It is minimum at small $I_{\rm dc}$ and increases with increasing $I_{\rm dc}$. The increase is nonmonotonic, presenting several peaks up to a current of the order of 1 μA, a sort of critical current above which the resistance is constant and independent of dc current. The many peaks in the differential resistance curves are typical of nonhomogeneous superconductivity. For instance the differential resistance jumps seen in narrow metal superconducting wires (diameter smaller than coherence length) are associated with the weak spots of the wire. Since neither the Pt/C electrodes nor the DNA molecules are superconducting (as shown in previous experiments), these results suggest that the gallium nanoparticles, which are superconducting, induce superconductivity through the DNA molecules. The superconducting transition temperature of pure gallium is $T_{\rm c} = 1$ K but it is reasonable to expect that the gallium nanoparticles, because of their small size and their probable large carbon content, have a higher $T_{\rm c}$ [19]. It is interesting to note that the low intrinsic carrier density in the DNA molecules may prevent the inverse proximity effect, i.e. the destruction of the superconductivity of the gallium nanoparticles. Those same nanoparticles could not induce any proximity effect in metallic wires because of the high density of carriers in metals. This possibility of inducing long-range superconductivity with superconducting nanoparticles was investigated recently in the context of graphene [18]. In the present case, it is very likely that those nanoparticles that transfer Cooper pairs at low temperature also transfer charge carriers through the DNA molecules above $T_{\rm c}$ (i.e. induce doping in the normal state).

The difference between the transitions of the various samples is probably related to the existence of nanoparticles of different sizes, leading to superconducting transitions more rounded and with a weaker $T_{\rm C}(H)$ dependence in small particles than in large ones. The radius R of the nanoparticles inducing superconductivity in DNA can be estimated from the critical field $H_{\rm c} = \Phi_0/\pi R^2$, for which the transition temperature extrapolates to 0. This field (see figure 4) is of the order of 10 T, corresponding to a radius between 5 and 7 nm. A rough estimate of the number of nanoparticles bound to DNA molecules participating in transport can also be deduced from the number of peaks of differential resistance, which varies between 3 and 6 depending on the samples (the largest number of peaks is observed in the lowest resistance samples). This corresponds to a typical distance between nanoparticles attached to a DNA molecule of the order of 10–20 nm, which is thus the length over which we probe electronic transport along the DNA molecules and not the total width of the slit. The relatively low values of measured resistances, as well as the appearance of proximity-induced superconductivity, indicate a strong electronic coupling between the DNA molecules and both Pt/C residues and Ga nanoparticles. The characteristic length over which the DNA molecules are doped by carrier injection from the gallium nanoparticles must be greater than or of the order of the length of a DNA molecule bridging two gallium nanoparticles, i.e. of the order of 10 nm. This contrasts with previous measurements of the DNA molecules linking gold nanoparticles [20], where the conductivity

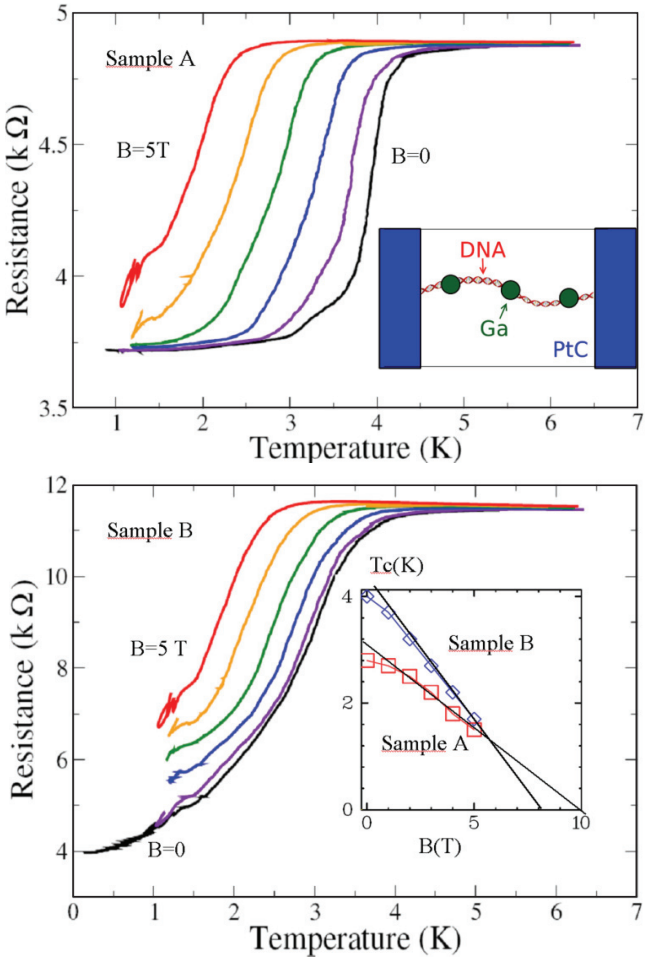

Figure 4. Low-temperature dependence at several magnetic fields (going from 0.1 to 5 T) of the resistance for two different samples where Ga nanoparticles are present inside the slit as sketched in the inset of the top panel. The inset of the bottom panel: magnetic field dependence of the critical temperature $T_c(H)$ deduced from the inflection points of the $R(T)$ curves.

did not exceed 10^{-4} S cm^{-1} for a distance between metallic nanoparticles of 10 nm, whereas the conductivity in the present case can be estimated to be of the order of unity in the same units. Accordingly, transport experiments on completely metallized DNA molecules [21] did not seem to indicate any intrinsic contribution of the DNA molecules to the conduction measured. These differences may originate from the nature of the binding between the metallic nanoparticles and the DNA, which in [20] was of covalent nature (involving alkanethiol molecules of low conductivity), whereas in the present case we believe that good electrical contact between DNA molecules and the metallic nanoparticles is provided by the discontinuities and defects in the pentylamine film. Our results indicate that DNA molecules ensure conduction between the electrodes since there is no conduction across the slits in the absence of these molecules. The Ga droplets constitute electron or Cooper pair reservoirs and can transfer charge carriers to the molecules if the metal–molecule electrical contact is sufficiently strong. As a result, instead of probing conduction along the molecules on distances of the order of 100 nm (the width of

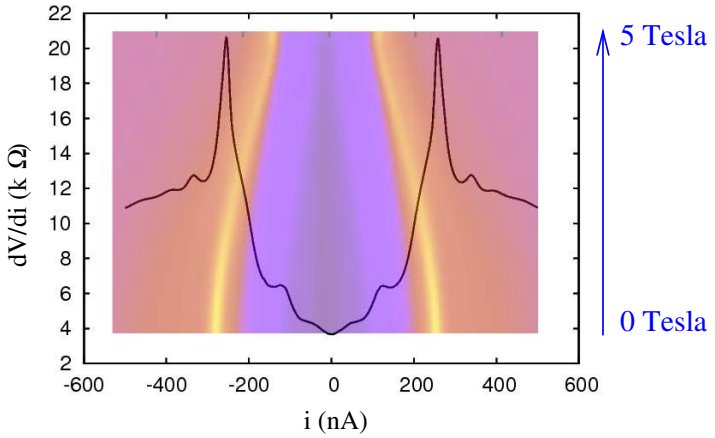

Figure 5. The black curve represents the differential resistance $\mathrm{d}V/\mathrm{d}I$ as a function of a dc current added to the small ac excitation current through sample B at 100 mK. The color inset in the background shows the evolution of the differential resistance encoded as a color scale, with yellow/violet representing maximal/minimal differential resistance. The x-axis represents the dc current as in the main figure, and the y-axis indicates the magnetic field ranging from 0 to 5 T.

the slit), we only probe this conduction on the typical distance between Ga nanoparticles, i.e. 10–20 nm. Thus, it is possible that the localization length of electronic wave functions along the DNA molecules does not exceed 20 nm. This length is enough to ensure the global connection of the network constituted by the nano-particles and the DNA molecules. Since in our previous experiments [15, 16] the DNA molecules were connected across similarly etched slits in thin metallic films, the existence of metallic residues cannot be excluded, and the conduction of DNA molecules could thus also have been probed on distances not greater than 10 nm. These results invite a systematic investigation on the possible carrier doping of DNA by metallic nanoparticles.

Acknowledgment

We thank F Livolant, A Leforestier, D Vuillaume and D Deresmes for fruitful discussions. We acknowledge ANR QuantADN and DGA for support.

References

[1] Arkin M R, Stemp E D A, Holmlin R E, Barton J K, Hoermann A, Olson E J C and Barbara P F 1996 *Science* **273** 475
Hall D B, Holmlin R E and Barton J K 1996 *Nature* **382** 731
[2] Tran P, Alavi B and Gruner G 2000 *Phys. Rev. Lett.* **85** 1564
[3] Fink H-W and Schönenberger C 1999 *Nature* **398** 407
[4] Porath D, Bezryadin A, de Vries S and Dekker C 2000 *Nature* **403** 635
[5] Endres R G, Cox D L and Singh R R P 2004 *Rev. Mod. Phys.* **76** 195
[6] Guo X, Gorodetsky A A, Hone J, Barton J K and Nuckolls C 2008 *Nat. Nanotechnol.* **3** 163

[7] Xu B, Zhang P, Li X and Tao N 2004 *Nano Lett.* **4** 1105
[8] Kang N, Erbe A and Scheer E 2008 *New J. Phys.* **10** 023030
Kang N, Erbe A and Scheer E 2010 *Appl. Phys. Lett.* **96** 023701
[9] Shapir E, Cohen H, Calzolari A, Cavazzoni C, Ryndyk D A, Cuniberti G, Kotlyar A, Di Felice R and Porath D 2008 *Nat. Mater.* **7** 68
[10] Wang J 2008 *Phys. Rev.* B **78** 245304
[11] Okahata Y *et al* 1998 *Supramol. Sci.* **5** 317
[12] Hartzell B *et al* 2003 *J. Appl. Phys.* **94** 2764
[13] Heim T, Deresmes D and Vuillaume D 2004 *Appl. Phys. Lett.* **85** 2637
Heim T, Deresmes D and Vuillaume D 2004 *J. Appl. Phys.* **96** 2927
[14] Mahapatro A K, Lee G U, Jeong K J and Janes D B 2009 *Appl. Phys. Let.* **95** 083106
[15] Kasumov A Y, Kociak M, Guéron S, Reulet B, Volkov V T, Klinov D V and Bouchiat H 2001 *Science* **291** 280
[16] Kasumov A Y, Klinov D V, Roche P-E, Guéron S and Bouchiat H 2004 *Appl. Phys. Lett.* **84** 1007
[17] Dubochet J, Ducommun M, Zollinger M and Kellenberger E 1971 *J. Ultrastruct. Res.* **35** 147
[18] Feigel'man M V, Skvortsov M A and Tikhonov K S 2009 *Solid State Commun.* **149** 1001
[19] Bakharev O N *et al* 2006 *Phys. Rev. Lett.* **96** 117002
[20] Park S-J *et al* 2000 *Angew. Chem.* **39** 3845
[21] Braun E, Eichen Y, Sivan U and Ben-Yoseph G 1998 *Nature* **391** 776